



*Original Article*

## Robust multi-model predictive control of multi-zone thermal plate system

Poom Jatunitanon<sup>1\*</sup>, Sarawoot Watechagit<sup>2</sup>, and Withit Chatlatanaguchai<sup>1</sup>

<sup>1</sup>Department of Mechanical Engineering, Faculty of Engineering, Kasetsart University, Chatuchak, Bangkok, 10900 Thailand

<sup>2</sup>Department of Mechanical Engineering, Faculty of Engineering, Mahidol University,  
Phutthamonthon, Nakhon Pathom, 73170 Thailand

Received: 18 May 2015; Revised: 9 October 2016; Accepted: 30 November 2016

---

### Abstract

A modern controller was designed by using the mathematical model of a multi-zone thermal plate system. An important requirement for this type of controller is that it must be able to keep the temperature set-point of each thermal zone. The mathematical model used in the design was determined through a system identification process. The results showed that when the operating condition is changed, the performance of the controller may be reduced as a result of the system parameter uncertainties. This paper proposes a weighting technique of combining the robust model predictive controller for each operating condition into a single robust multi-model predictive control. Simulation and experimental results showed that the proposed method performed better than the conventional multi-model predictive control in rise time of transient response, when used in a system designed to work over a wide range of operating conditions.

**Keywords:** robust multi-model predictive control, conventional model predictive control, weighting techniques, multi-zone thermal plates, bake plate system

---

### 1. Introduction

The design objective of a model predictive control (MPC) generally uses a linear model to compute the trajectory of future control inputs when optimizing the future behavior of the system outputs over a limited time window. However, when the system operating conditions are changed, model uncertainty could lower the controller performance. To minimize the impact of uncertainties in a system designed to operate in a wide range of operating conditions, a multi-model controller algorithm might offer a possible solution to the problem.

Literature reviews revealed that a number of techniques using a multi-model controller algorithm have been proposed to control different systems. For example, Dougherty and Cooper (2003) proposed a multiple model

adaptive control for a multivariable model predictive control by designing a model predictive algorithm for each operating condition and using output variables to choose the suitable controller for a multi-tank and distillation column system. Chen *et al.* (2009) designed a multiple model predictive control for an electric car fuel cell based on the variation of vehicle loads. Gan and Wang (2011), in their implementation of a multi-model predictive control in an induction motor, classified the system into low-speed and high-speed models and designed a model predictive control for each model. They also compared the two switching strategies otherwise known as the bumpless transfer switching and the hysteresis switching strategies. Experimental results have also shown that the hysteresis switching method had better closed-loop performance than the bumpless transfer switching method.

The requirement for a controller of a multi-zone thermal plate or bake plate system, also known as multi-input multi-output system, is that it must be able to keep a temperature at a set-point in each thermal zone. Several techniques to control such systems have been proposed in the literature. For example, Hoa *et al.* (2007) proposed a

---

\*Corresponding author

Email address: [poom\\_legend@hotmail.com](mailto:poom_legend@hotmail.com)

decentralized controller with feed-forward proportional-integral in each of the multi-zone thermal plates. Experimental results showed that the feed-forward part did improve the system transient response. In their simulation study of the predictive ratio control, Tay *et al.* (2008) showed that the strategy was able to improve the performance of the two-zone thermal plate system.

Ling *et al.* (2009) proposed the multiplexed model predictive control to reduce the computational time of a model predictive control in multi-zone thermal plates using speedily updated information of the system control input, output response, disturbance signal, and reference signal.

The literature reviews also revealed that many more research studies have developed control algorithms to deal with transient performance, computational time reduction, and plant uncertainty handling over a wide range of operating conditions. This therefore shows that the multi-zone thermal plate system needs a controller with a multivariable framework to deal with the multivariable problems and model uncertainties that are associated with the different operating conditions.

This paper presents the first time implementation of a robust multi-model predictive controller with weighting techniques for a multi-zone thermal plate system. While most of multi-zone thermal plate controllers are designed based on a single point of the plant model, the proposed controller is designed from an uncertain model by using the linear matrix inequality algorithm in predictive control framework. Due to the wide range of operating conditions, each of the robust model predictive controllers has been combined into the robust multi-model predictive controller by using weighting techniques. To guarantee stability of the closed-loop system,

this paper studied the stability of the multi-model with an uncertain system using Lyapunov’s direct method.

The remaining sections of this paper include the Materials and Methods section, which discusses the basics of the model predictive control, the robust model predictive control, the method for dividing the range of operating conditions into sub-models, the bank of the controller and the stability analysis of a multi-model system, the weighting method for creating the multi-model predictive control for each model predictive controller under each operating condition, and finally the experimental set-up. This is followed by the Results and Discussion section, which presents the results of the simulation and experimental study, while the final section concludes the paper.

## 2. Materials and Methods

### 2.1 Conventional model predictive control

The steps of Maciejowski (2002) for developing the MPC were followed in this study. For solving the predictive control problem, the controller must compute the predicted values of the state vector  $\hat{x}(k+i|k)$  from the measurement of the current state vector  $x(k|k)$ , the latest input  $u(k-1)$ , and the future input changes,  $\Delta u(k+i|k)$ . The notation  $(k+i|k)$  indicates that the parameter at time  $(k+i)$  depends on the conditions at current time step  $k$ . The future of the predicted state vector can then be calculated sequentially using the set of future control parameters as in equation (1):

$$\begin{bmatrix} \hat{x}(k+1|k) \\ \vdots \\ \hat{x}(k+N_c|k) \\ \hat{x}(k+N_c+1|k) \\ \vdots \\ \hat{x}(k+N_p|k) \end{bmatrix} = \begin{bmatrix} A \\ \vdots \\ A^{N_c} \\ A^{N_c+1} \\ \vdots \\ A^{N_p} \end{bmatrix} x(k) + \begin{bmatrix} B \\ \vdots \\ \sum_{i=0}^{N_c-1} A^i B \\ \sum_{i=0}^{N_c} A^i B \\ \vdots \\ \sum_{i=0}^{N_p-1} A^i B \end{bmatrix} u(k-1) + \begin{bmatrix} B & \cdots & 0 \\ (A+I)B & \cdots & 0 \\ \vdots & \ddots & \vdots \\ \sum_{i=0}^{N_c-1} A^i B & \cdots & B \\ \sum_{i=0}^{N_c} A^i B & \cdots & (A+I)B \\ \vdots & \vdots & \vdots \\ \sum_{i=0}^{N_p-1} A^i B & \cdots & \sum_{i=0}^{N_p-N_c} A^i B \end{bmatrix} \begin{bmatrix} \Delta u(k|k) \\ \vdots \\ \Delta u(k+N_c-1|k) \end{bmatrix} \quad (1)$$

where matrix A and B are the system matrix and the control input matrix. The parameters  $N_p$  and  $N_c$  are used to capture the future of the predicted state vector and control input trajectory. The control horizon  $N_c$  is chosen to be less than or equal to the prediction horizon  $N_p$ . When the whole state vector is measured,  $\hat{x}(k|k) = x(k) = y(k)$  or the output matrix  $C = I$ . The sequential output variable can thus be rewritten into a compact matrix form as in equation (2):

$$Y(k) = \Psi x(k) + \Upsilon u(k-1) + \Theta \Delta U(k) \quad (2)$$

where  $Y(k) = [y(k+1|k), \dots, y(k+N_c|k), y(k+N_c+1|k), \dots, y(k+N_p|k)]^T$  is a vector of the predicted output and  $\Delta U(k) = [\Delta u(k|k), \dots, \Delta u(k+N_c-1|k)]^T$  is a vector of the future input changes. The matrix  $\Psi$ ,  $\Upsilon$  and  $\Theta$  can be written as:

$$\Psi = \begin{bmatrix} CA \\ \vdots \\ CA^{N_c} \\ CA^{N_c+1} \\ \vdots \\ CA^{N_p} \end{bmatrix}, \Upsilon = \begin{bmatrix} CB \\ \vdots \\ C(\sum_{i=0}^{N_c-1} A^i B) \\ C(\sum_{i=0}^{N_c} A^i B) \\ \vdots \\ C(\sum_{i=0}^{N_p-1} A^i B) \end{bmatrix}, \Theta = \begin{bmatrix} CB & \cdots & 0 \\ C(A+I)B & \cdots & 0 \\ \vdots & \ddots & \vdots \\ C(\sum_{i=0}^{N_c-1} A^i B) & \cdots & CB \\ C(\sum_{i=0}^{N_c} A^i B) & \cdots & C(A+I)B \\ \vdots & \vdots & \vdots \\ C(\sum_{i=0}^{N_p-1} A^i B) & \cdots & C(\sum_{i=0}^{N_p-N_c} A^i B) \end{bmatrix} \quad (3)$$

The cost function, defined as  $J(k)$ , reflects the control objective and is expressed as equation (4):

$$J(k) = \|\Gamma(k) - Y(k)\|_Q^2 + \|\Delta U(k)\|_R^2 \quad (4)$$

where  $\Gamma(k) = [r(k+1|k), \dots, r(k+N_p|k)]^T$  is a vector of the reference signal. The notation  $\|\bullet\|_Q^2 = [\bullet]^T Q [\bullet]$  and  $\|\bullet\|_R^2 = [\bullet]^T R [\bullet]$ . The first term represents the objective of minimizing the prediction error. The second term reflects the consideration given to the size of the future input changes when the cost function is minimized. The weight matrices  $Q$  and  $R$  are positive definite matrices for tuning the closed-loop performance. The tracking error can be written as equation (5):

$$E(k) = \Gamma(k) - \underbrace{\Psi x(k) + \Upsilon u(k-1) - \Theta \Delta U(k)}_{Y(k)} \quad (5)$$

The controller must keep the tracking error to zero, then the control input tends to a constant value or the input change is zero. Therefore, the reference signal can be rewritten as equation (6):

$$\Gamma(k) = E(k) + \Psi x(k) + \Upsilon u(k-1) \quad (6)$$

The cost function from equation (4) became equation (7) by substituting the reference signal in equation (6) and a compact matrix form of the sequential output variable in equation (2) into the cost function as shown in equation (7):

$$\begin{aligned} J(k) &= \|\underbrace{E(k) + \Psi x(k) + \Upsilon u(k-1)}_{Y(k)} - (\Psi x(k) + \Upsilon u(k-1) + \Theta \Delta U(k))\|_Q^2 + \|\Delta U(k)\|_R^2 \\ &= \|E(k) - \Theta \Delta U(k)\|_Q^2 + \|\Delta U(k)\|_R^2 \\ &= [E(k)^T - \Theta^T \Delta U(k)^T] Q [E(k) - \Delta U(k) \Theta] + \Delta U(k)^T R \Delta U(k) \\ &= E(k)^T Q E(k) - 2 \Delta U(k)^T \Theta^T Q E(k) + \Delta U(k)^T [\Theta^T Q \Theta + R] \Delta U(k) \end{aligned} \quad (7)$$

Taking the first derivative of the cost function in equation (7) is shown in equation (8):

$$\frac{\partial J(k)}{\partial \Delta U(k)} = 2 \Theta^T Q E(k) + 2 [\Theta^T Q \Theta + R] \Delta U(k) \quad (8)$$

To check the minimum fixed points, the second derivative of the cost function in equation (7) is shown in equation (9):

$$\frac{\partial^2 J(k)}{\partial \Delta U(k)^2} = 2 (\Theta^T Q \Theta + R) \quad (9)$$

The weight matrices  $Q$  and  $R$  are positive definite matrices. Therefore,  $\Theta^T Q \Theta + R > 0$  then the second derivative is certainly positive definite, which is enough to guarantee minimum fixed points.

The minimal solution for a control signal can be determined by setting the first derivative to zero, then the minimal control signal can thus be written as equation (10):

$$\Delta U(k) = -[\Theta^T Q \Theta + R]^{-1} \Theta^T Q E(k) \quad (10)$$

In general, only the first control input is implemented. Therefore, the controller gain can be written as equation (11):

$$K_{MPC} = -[I \ 0 \ \dots \ 0](\Theta^T Q \Theta + R)^{-1} \Theta^T Q \tag{11}$$

For implementation in a tracking system, the controller gain for tracking systems can be calculated by equation (12). The implementation needs the information of all state variables, the reference signal, and the latest control input.

$$\Delta U(k)_{opt} = K_{MPC} \begin{bmatrix} I \\ I \\ \vdots \\ I \end{bmatrix}, \Psi, Y \begin{bmatrix} \Gamma(k) \\ x(k) \\ u(k-1) \end{bmatrix} \tag{12}$$

The general settings of the time limit steps are  $N_c \geq n$  and  $N_p \geq 2n$ , where  $n$  is the number of states in the plants. The reason for making  $N_p \geq 2n$  is to have a sufficiently long costing interval. This ensures that the output remains at zero for at least  $n$  steps and the error signals do not start entering the cost function until the set-point has been achieved exactly.

In the case of disturbance problems, equation (1) can be rewritten as equation (13):

$$\begin{aligned} y(k+i|k) &= C\hat{x}(k+i|k) + Du(k+i|k) \\ &= C\hat{x}(k+i|k) + D \left[ u(k-1) + \sum_{j=0}^i \Delta u(k+j|k) \right] \end{aligned} \tag{13}$$

where  $D$  is the disturbance matrix. The set of future outputs from time step  $k+1$  to time step  $k+N_p$  can be written as:

$$\begin{aligned} \begin{bmatrix} y(k+1|k) \\ \vdots \\ y(k+N_p|k) \end{bmatrix} &= \begin{bmatrix} C & 0 & \dots & 0 \\ 0 & C & \dots & 0 \\ \vdots & \vdots & \ddots & \vdots \\ 0 & 0 & \dots & C \end{bmatrix} \begin{bmatrix} \hat{x}(k+1|k) \\ \vdots \\ \hat{x}(k+N_p|k) \end{bmatrix} + \begin{bmatrix} D \\ \vdots \\ D \end{bmatrix} u(k-1) \\ &+ \begin{bmatrix} D & D & 0 & \dots & 0 \\ \vdots & \vdots & \vdots & \ddots & \vdots \\ D & D & D & \dots & D \end{bmatrix} \begin{bmatrix} \Delta u(k|k) \\ \Delta u(k+1|k) \\ \vdots \\ \Delta u(k+N_p|k) \end{bmatrix} \end{aligned} \tag{14}$$

**2.2 Robust model predictive control**

The development of robust model predictive control in this study is based on the work of Kothare *et al.* (1996). The advantage of robust model predictive control (RMPC) is its ability to deal with plant model uncertainties. Such a model may be represented by a state-space with polytopic uncertainty as expressed in equation (15):

$$\begin{aligned} x(k+1) &= A_{n_i}x(k) + B_{n_i}u(k) \\ \Omega &\in [A_{n_i}, B_{n_i}] \\ \Omega &= Co[(A_{n_1}, B_{n_1}), (A_{n_2}, B_{n_2}), \dots, (A_{n_L}, B_{n_L})] \end{aligned} \tag{15}$$

where  $\Omega$  is the polytope,  $Co$  denotes the convex hull, and  $[A_{n_i}, B_{n_i}]$  are the vertices of the convex hull.

The nominal performance objective is defined as:

$$J_\infty(k) = \sum_{i=0}^{\infty} \|\tilde{y}(k+i|k)\|_Q^2 + \|\Delta u(k+i|k)\|_R^2 \tag{16}$$

where  $J_\infty(k) = \sum_{i=0}^{\infty} \|\tilde{y}(k+i|k)\|_Q^2 + \|\Delta u(k+i|k)\|_R^2$  is an error signal from the reference and measured output signal.

The selection of the  $N_p$  and  $N_c$  values sometimes leads to poor nominal stability properties. Therefore, it is preferable to adopt

the infinite horizon approach to guarantee at least nominal stability. The proof of nominal stability followed Maciejowski (2002), based on measurement of all state variables when the plant is stable, the model is perfect, the model has no disturbances and all of the weight matrices are positive definite.

**Proof.** From the cost function (16), we want to drive the error to zero:

$$J_{\infty}(k) = \sum_{i=1}^{\infty} \left\{ \|\tilde{y}(k+i|k)\|_Q^2 + \|\Delta u(k+i-1|k)\|_R^2 + \|u(k+i-1|k)\|_S^2 \right\} \quad (17)$$

The first  $N_c$  control moves are non-zero:  $\Delta u(k+i-1|k)=0$  for  $i > N_c$  and we assume the weight matrix  $S > 0, Q > 0$  and  $R > 0$ . Then the closed-loop stability is obtained for any  $N_c > 0$ , providing that the global optimum is found at each step. Let  $J^0(k)$  be the optimal value of the cost function at time  $k$ ,  $u^0$  denote the computed optimal input level and  $\tilde{y}$  denote values of the error obtained as a result of applying  $u^0$ . Since,  $u^0(k+i) = u^0(k+N_c-1)$  for  $i \geq N_c$ , and since the steady-state value of  $u^0$  needs to keep  $\tilde{y}$  at zero, the optimizer will certainly put  $u^0(k+i) = 0$  for  $i \geq N_c$ , since an infinite cost would otherwise result. Thus we have

$$J^0(k) = \sum_{i=1}^{\infty} \|\tilde{y}(k+i|k)\|_Q^2 + \sum_{i=1}^{N_c} \left\{ \|\Delta u^0(k+i-1|k)\|_R^2 + \|u^0(k+i-1|k)\|_S^2 \right\} \quad (18)$$

The value of  $J$ , evaluated at time  $k+1$ , but maintaining the same control sequence  $u^0(k+i|k)$  as computed at time  $k$ , would be

$$J(k+1) = J^0(k) - \|\tilde{y}^0(k+1)\|_Q^2 - \|\Delta u^0(k|k)\|_R^2 - \|\Delta u^0(k|k)\|_S^2 \quad (19)$$

However, at time  $k+1$  the optimization problem becomes:

$$\begin{aligned} J^0(k+1) &\leq J(k+1) \\ &= J^0(k) - \|\tilde{y}^0(k+1)\|_Q^2 - \|\Delta u^0(k|k)\|_R^2 - \|\Delta u^0(k|k)\|_S^2 \\ &< J^0(k) \end{aligned} \quad (20)$$

To infer stability we must now show that  $J^0(k+1) \leq J^0(k)$  implies that  $\|\tilde{y}\|$  is decreasing. By minimization of the robust performance objective, the following is illustrated:

$$\min_{u(k+i|k) \in K_{\text{RMPC}} \tilde{y}(k+i|k)} \max_{[A_m, B_m] \in \Omega} J_{\infty}(k) \quad (21)$$

We address the nominal performance objective by first deriving an upper bound of the worst case performance cost. We assume that at each sampling time  $k$ , a control law  $u(k+i|k) = K_{\text{RMPC}} \tilde{y}(k+i|k)$  is used to minimize the value of  $J_{\infty}(k)$ . At sampling time  $k$ , we define a quadratic function  $V(\tilde{y}(k)) = \tilde{y}^T(k)P(k)\tilde{y}(k), P > 0$ . For any  $[A_m, B_m] \in \Omega$ , we suppose  $V(\tilde{y}(k))$  satisfies the following robust stability constraint:

$$V(\tilde{y}(k+i+1|k)) - V(\tilde{y}(k+i|k)) \leq -\left[ \tilde{y}(k+i|k)^T Q \tilde{y}(k+i|k) + u(k+i|k)^T R u(k+i|k) \right] \quad (22)$$

Summing equation (22) from  $i=0$  to  $\infty$  and requiring  $\tilde{y}(\infty|k) = 0$  or,  $V(\tilde{y}(\infty|k)) = 0$  we get

$$\max_{[A_m, B_m] \in \Omega} J_{\infty}(k) \leq V(\tilde{y}(k|k)) \leq \gamma \quad (23)$$

The condition  $V(\tilde{y}(k|k)) \leq \gamma$  can be expressed equivalently as the linear matrix inequality (LMI) (24):

$$\begin{bmatrix} \gamma & \tilde{y}(k|k)^T \\ \tilde{y}(k|k) & \psi \end{bmatrix} \geq 0, \psi > 0 \tag{24}$$

where  $\psi = P(k)^{-1}$ . The robust stability constraint (22) can be expressed equivalently as the LMI:

$$\begin{bmatrix} \psi & \psi A_{ni}^T + Y^T B_{ni}^T & \psi Q^{1/2} & Y^T R^{1/2} \\ A_{ni} \psi + B_{ni} Y & \psi & 0 & 0 \\ Q^{1/2} \psi & 0 & \gamma I & 0 \\ R^{1/2} Y & 0 & 0 & \gamma I \end{bmatrix} \geq 0, i \in (1, 2, \dots, l) \tag{25}$$

The parameters  $\psi$  and  $Y$  are obtained from the LMI solution by using the LMI control toolbox (Gahinet *et al.*, 1995).

The robust controller gain ( $K_{\text{RMPC}}$ ) in the control input  $u(k+i|k) = K_{\text{RMPC}} \tilde{y}(k+i|k)$ ,  $i \geq 0$  that minimizes the upper bound  $V(\tilde{y}(k))$  of the robust performance objective function, is given by

$$K_{\text{RMPC}} = Y \psi^{-1} \tag{26}$$

The robust controller gain can be synthesized by substituting the vector of the operating conditions into the inequality (24) and then solving for the LMI problems (24) and (25) from the LMI toolbox.

### 2.3 Multi-zone thermal plate system

The multi-zone thermal plate system is used for heating or cooling a wafer plate over a period in a semiconductor process. In general, the shape of the multi-zone thermal plates is circular and the thermal zone is divided into cylindrical coordinates. The center of a plate is referred to as the first thermal zone and the next thermal zones are separated by annular spaces in the plate. This work set-up at the demo system of a multi-zone thermal plate in the Cartesian coordinates is shown in Figure 1. Each zone of the multi-zone thermal plate contains one thermoelectric module (size 4 cm<sup>2</sup>). The set-up in the Cartesian coordinates uses the same power source in each thermoelectric module while in the cylindrical coordinate set-up, a high power source level was used in the first thermal zone which is then reduced as annular spaces increase in the plate. A large heat sink and two fans were used to remove heat stored on the other side of the four thermoelectric modules. This system has four-input voltages applied to each thermoelectric module and four-output temperatures in each zone. Each zone is fitted with a thermocouple type K to measure the temperature signal.

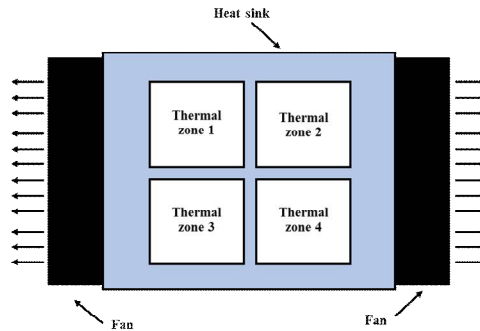


Figure 1. Multi-zone thermal plate system.

### 2.4 Map of the system behavior

Tan *et al.* (2004) proposed the idea of operating point selection in a multi-model controller using a steady-state map. A steady-state map is drawn from the data of the steady-state inputs and steady-state outputs of a system. In this study, the average value of the four input and four output signals was used to draw the steady-state map (Figure 2). The entire system was separated into three subsystem regions: the first subsystem covered an average temperature range of 23 °C to 70 °C of the multi-zone thermal plates system; the second covered a temperature range of 71 °C to 121 °C, and the last region had temperatures ranging from 121 °C to 124 °C. Each operating region had a system matrix and control input matrix following the step response model process of Maciejowski (2002). All parameters of the system matrix and control input matrix are presented in Table 1.

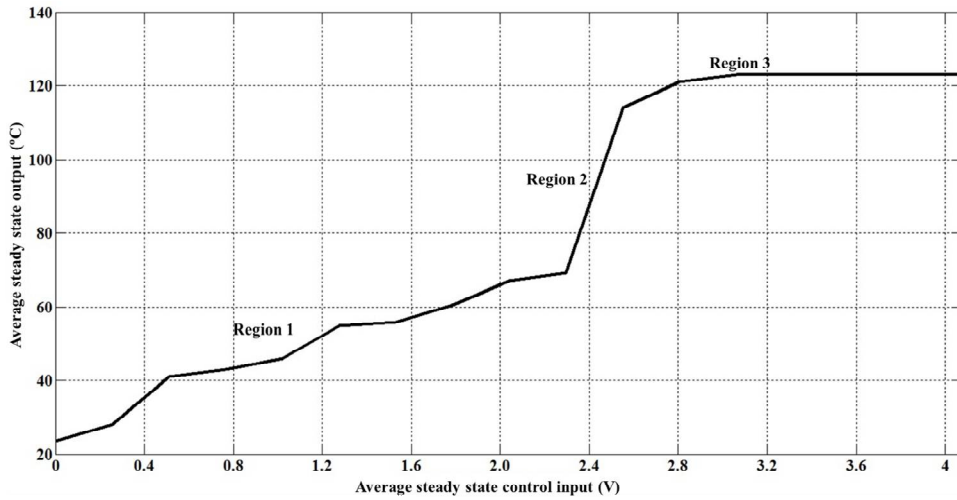


Figure 2. Steady-state map of a multi-zone thermal plate system.

Table 1. Parameters of the system matrix and control input matrix in each region.

Region	System matrix ( $A_{ni}$ )	Control input matrix ( $B_{ni}$ )
$18^{\circ}\text{C} \leq T_{\text{aver}} \leq 70^{\circ}\text{C}$	$\begin{bmatrix} 0.9009 & 0.066 & -0.0896 & 0.0809 \\ 0.2354 & 0.6097 & -0.0357 & 0.1415 \\ 0.0851 & 0.0402 & 0.5237 & 0.2752 \\ 0.0759 & 0.0317 & 0.0944 & 0.7864 \end{bmatrix}$	$\begin{bmatrix} 0.0124 & 0.0021 & -0.003 & -0.001 \\ 0.0029 & 0.0469 & -0.014 & -0.002 \\ 0.0007 & 0.0005 & 0.0441 & -0.005 \\ 0.0006 & 0.0016 & 0.0035 & -0.024 \end{bmatrix}$
$71^{\circ}\text{C} \leq T_{\text{aver}} \leq 121^{\circ}\text{C}$	$\begin{bmatrix} 0.8666 & 0.0038 & -0.0181 & 0.1143 \\ 0.1430 & 0.6478 & 0.0133 & 0.1653 \\ 0.0589 & -0.005 & 0.7274 & 0.1484 \\ 0.0857 & 0.1021 & 0.0579 & 0.7688 \end{bmatrix}$	$\begin{bmatrix} 0.0229 & -0.001 & -0.004 & -0.007 \\ 0.0015 & 0.0192 & 0.0002 & -0.001 \\ 0.0008 & 0.0001 & 0.0125 & -0.012 \\ 0.0014 & 0.0015 & 0.0010 & -0.096 \end{bmatrix}$
$121^{\circ}\text{C} \leq T_{\text{aver}} \leq 124^{\circ}\text{C}$	$\begin{bmatrix} 0.8812 & -0.078 & -0.004 & 0.1633 \\ 0.0978 & 0.6559 & 0.0060 & 0.2014 \\ 0.0857 & 0.0274 & 0.6892 & 0.1644 \\ 0.1425 & 0.1465 & 0.0139 & 0.7202 \end{bmatrix}$	$\begin{bmatrix} 0.0228 & -0.001 & -0.001 & -0.005 \\ 0.0012 & 0.0177 & -0.003 & -0.008 \\ 0.0009 & 0.0003 & 0.0073 & -0.004 \\ 0.0019 & 0.0014 & -0.002 & -0.009 \end{bmatrix}$

From Table 1, we define the upper bound of system matrix  $\bar{A}$  and control input matrix  $\bar{B}$  through equation (27):

$$\bar{A} = \begin{bmatrix} 0.9009 & 0.0660 & -0.0040 & 0.1633 \\ 0.2354 & 0.6559 & 0.0133 & 0.2014 \\ 0.0857 & 0.0402 & 0.7274 & 0.2752 \\ 0.1425 & 0.1465 & 0.0944 & 0.7894 \end{bmatrix}, \bar{B} = \begin{bmatrix} 0.0229 & 0.0021 & -0.0010 & -0.001 \\ 0.0029 & 0.0469 & 0.0002 & -0.001 \\ 0.0009 & 0.0005 & 0.0441 & -0.004 \\ 0.0019 & 0.0016 & 0.0035 & -0.009 \end{bmatrix} \quad (27)$$

where all of the elements in matrices  $\bar{A}$  and  $\bar{B}$  are the maximum values in every element of the matrix in Table 1. We defined the lower bound of the system matrix  $\underline{A}$  and control input matrix  $\underline{B}$  as equation (28). The minimum values of every element in all matrices in Table 1 are contained in a lower bound matrix.

$$\underline{A} = \begin{bmatrix} 0.8666 & -0.0780 & -0.0896 & 0.0809 \\ 0.0978 & 0.6097 & -0.0357 & 0.1415 \\ 0.0589 & -0.0050 & 0.5237 & 0.1484 \\ 0.0759 & 0.0317 & 0.0139 & 0.7202 \end{bmatrix}, \underline{B} = \begin{bmatrix} 0.0124 & -0.001 & -0.004 & -0.007 \\ 0.0012 & 0.0177 & -0.014 & -0.008 \\ 0.0007 & 0.0001 & 0.0073 & -0.012 \\ 0.0006 & 0.0014 & -0.002 & -0.096 \end{bmatrix} \quad (28)$$

The bound of uncertainties of the system matrix and control input matrix in every subsystem can thus be calculated by equation (29):

$$\Xi_{Ai} = (A_{ni} - A_{\text{nom}}) \times A_{\text{dev}}^{-1}, \Xi_{Bi} = (B_{ni} - B_{\text{nom}}) \times B_{\text{dev}}^{-1} \quad (29)$$

where  $A_{nom} = \frac{1}{2}(\bar{A} + \underline{A})$  and  $A_{dev} = \frac{1}{2}(\bar{A} - \underline{A})$ . The uncertainty matrices of the system matrix and control input matrix are presented in equations (30) and (31), respectively:

$$\Xi_{A1} = \begin{bmatrix} 1 & 1 & -1 & -1 \\ 1 & -1 & -1 & -1 \\ 1 & 1 & -1 & 1 \\ -1 & -1 & 1 & 1 \end{bmatrix}, \Xi_{A2} = \begin{bmatrix} -1 & 0.1 & 0.7 & -0.2 \\ -0.3 & 0.7 & 1 & -0.2 \\ -1 & -1 & 1 & -1 \\ -0.7 & 0.2 & 0.1 & 0.4 \end{bmatrix}, \Xi_{A3} = \begin{bmatrix} -0.2 & -1 & 1 & 1 \\ -1 & 1 & 0.7 & 1 \\ 1 & 0.4 & 0.6 & -0.8 \\ 1 & 1 & -1 & -1 \end{bmatrix} \quad (30)$$

$$\Xi_{B1} = \begin{bmatrix} -1 & 1 & -0.3 & 1 \\ 1 & 1 & -1 & 0.7 \\ -1 & 1 & 1 & 0.8 \\ -1 & 1 & 1 & 0.7 \end{bmatrix}, \Xi_{B2} = \begin{bmatrix} 1 & -1 & -1 & -1 \\ -0.7 & -0.9 & 1 & 1 \\ 0 & -1 & -0.7 & -1 \\ 0.2 & 0 & 0.1 & -1 \end{bmatrix}, \Xi_{B3} = \begin{bmatrix} 1 & -1 & 1 & -0.3 \\ -1 & -1 & 0.6 & -1 \\ 1 & 0 & -1 & 1 \\ 1 & -1 & -1 & 1 \end{bmatrix} \quad (31)$$

### 2.5 Controller bank

For a demonstration of the performance of the proposed control system, diagrams of the proposed controller and multi-zone thermal plate are shown in Figure 3.

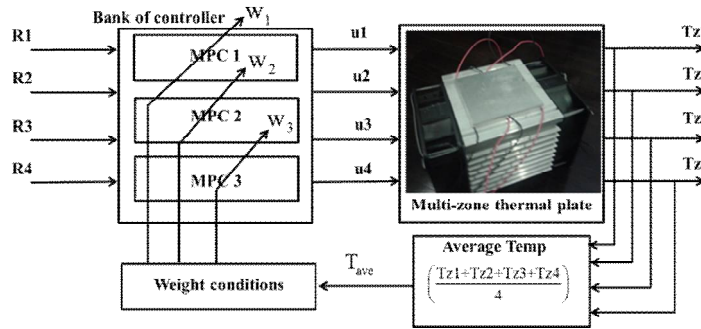


Figure 3. Diagram of the proposed control system.

The control effort in each thermal zone can be written as

$$u_{1,2,3,4} = \left( \sum_{i=1}^3 w_i(k) MPC_i \right) / \sum_{i=1}^3 w_i(k) \quad (32)$$

where  $i = 1, 2$  and  $3$  are the numbers of the local controllers from regions one, two, and three, respectively. The weight parameters  $w_1, w_2$  and  $w_3$  are used to share the effects of each local model predictive controller according to an average temperature. The state equation of a multi-model with uncertainties can thus be written as:

$$x(k+1) = \sum_{i=1}^L w_i(k) \left[ \overbrace{\left( A_{nom} + (\Xi_{Ai} \otimes A_{dev}) \right)}^{A_u} x(k) + \overbrace{\left( B_{nom} + (\Xi_{Bi} \otimes B_{dev}) \right)}^{B_u} u(k) \right] / \sum_{i=1}^L w_i(k) \quad (33)$$

$$\Xi_{Ai} \in [-1 \ 1], \Xi_{Bi} \in [-1 \ 1]$$

where the nomenclature  $\otimes$  refers to the product of the matrix in the element-by-element method, and parameter  $L$  is the total number of all subsystems. The closed-loop system of equation (33) can thus be determined by substituting the control law  $u(k) = -K_i x(k)$  into equation (33), so the closed-loop system becomes equation (34).

$$x(k+1) = \sum_{i=1}^L w_i(k) \left[ \underbrace{\left( A_{nom} - K_i B_{nom} \right)}_{\text{Nominal part}} + \underbrace{\left( (\Xi_{Ai} \otimes A_{dev}) - K_i (\Xi_{Bi} \otimes B_{dev}) \right)}_{\text{Uncertain part}} \right] x(k) / \sum_{i=1}^L w_i(k) \quad (34)$$

The first part of a closed-loop equation refers to the nominal part, whereas the second part represents the uncertain part. The state feedback gain  $K_i$  is used to handle the nominal and uncertain parts. If we define the parameter of the closed-loop system as:  $\tilde{Q}_i = (A_{nom} - K_i B_{nom}) + ((\Xi_{Ai} \otimes A_{dev}) - K_i (\Xi_{Bi} \otimes B_{dev}))$ , the equation can thus be simplified as equation (35):

$$x(k+1) = \sum_{i=1}^L w_i(k) \tilde{Q}_i x(k) / \sum_{i=1}^L w_i(k) \tag{35}$$

**2.6 Robust stability analysis**

The steps for deriving the stability of the multi-model with uncertainty system were obtained using Lyapunov’s direct method.

**Theorem 1.** Based on the proposal of Tanaka and Sugeno (1992), a discrete system described by  $x(k+1) = f(x(k))$ , where  $x(k) \in R^n$ ,  $f(x(k))$  is a function vector with the defined property:  $f(0) = 0$  for all  $k$ . Supposing there exists a scalar function  $V(x(k))$  continuous in  $x(k)$  such that  $V(0) = 0$ ,  $V(x(k)) > 0$  for  $x(k) \neq 0$ , when  $V(x(k))$  approaches infinity as  $\|x(k)\| \rightarrow \infty$  and  $\Delta V(x(k)) < 0$  for  $x(k) \neq 0$ , then the equilibrium state  $x(k) = 0$  for all  $k$  would be asymptotically stable with  $V(x(k))$  as the Lyapunov function. Considering the scalar function  $V(x(k)) = x^T(k) P x(k)$ , where  $P$  is a positive definite matrix, the decrease of the Lyapunov function can then be derived as:

$$\begin{aligned} \Delta V(x(k)) &= V(x(k+1)) - V(x(k)) \\ &= x^T(k+1) P x(k+1) - x^T(k) P x(k) \\ &= \left( \sum_{i=1}^L w_i(k) \tilde{Q}_i x(k) / \sum_{i=1}^L w_i(k) \right)^T P \left( \sum_{i=1}^L w_i(k) \tilde{Q}_i x(k) / \sum_{i=1}^L w_i(k) \right) - x^T(k) P x(k) \\ &= x^T(k) \left[ \left( \sum_{i=1}^L w_i(k) \tilde{Q}_i^T / \sum_{i=1}^L w_i(k) \right) P \left( \sum_{i=1}^L w_i(k) \tilde{Q}_i / \sum_{i=1}^L w_i(k) \right) - P \right] x(k) \\ &= \sum_{i,j=1}^L w_i(k) w_j(k) x^T(k) (\tilde{Q}_i^T P \tilde{Q}_j - P) x(k) / \sum_{i,j=1}^L w_i(k) w_j(k) \\ &= \left[ \sum_{i=1}^L (w_i(k))^2 x^T(k) (\tilde{Q}_i^T P \tilde{Q}_i - P) x(k) \right. \\ &\quad \left. + \sum_{i \neq j} w_i(k) w_j(k) x^T(k) (\tilde{Q}_i^T P \tilde{Q}_j + \tilde{Q}_j^T P \tilde{Q}_i - 2P) x(k) \right] / \sum_{i,j=1}^L w_i(k) w_j(k), \end{aligned}$$

where  $w_i(k) \geq 0$  for  $i \in (1, 2, \dots, L)$  and  $\sum_{i,j=1}^L w_i(k) w_j(k) > 0$ .

**Lemma 1.** If  $P$  is a positive definite matrix such that  $\tilde{Q}_i^T P \tilde{Q}_i - P < 0$  and  $\tilde{Q}_j^T P \tilde{Q}_j - P < 0$ , where  $\tilde{Q}_i, \tilde{Q}_j, P \in R^{n \times n}$ , then  $\tilde{Q}_i^T P \tilde{Q}_j + \tilde{Q}_j^T P \tilde{Q}_i - 2P < 0$

**Proof.**

$$\begin{aligned} \tilde{Q}_i^T P \tilde{Q}_j + \tilde{Q}_j^T P \tilde{Q}_i - 2P &= -(\tilde{Q}_i - \tilde{Q}_j)^T P (\tilde{Q}_i - \tilde{Q}_j) + \tilde{Q}_i^T P \tilde{Q}_i + \tilde{Q}_j^T P \tilde{Q}_j - 2P \\ &= -(\tilde{Q}_i - \tilde{Q}_j)^T P (\tilde{Q}_i - \tilde{Q}_j) + \tilde{Q}_i^T P \tilde{Q}_i - P + \tilde{Q}_j^T P \tilde{Q}_j - P \end{aligned}$$

Since  $P$  is a positive definite matrix, the term  $-(\tilde{Q}_i - \tilde{Q}_j)^T P (\tilde{Q}_i - \tilde{Q}_j) \leq 0$ , then the conclusion of the lemma follows.

**Theorem 2.** Based on the proposal of Tanaka and Sugeno (1992), the equilibrium of a multi-model with uncertainties system is globally asymptotically stable if there exists a common positive definite matrix  $P$  for all the subsystems such that:

$$\tilde{Q}_i^T P \tilde{Q}_i - P < 0 \text{ for } i \in (1, 2, \dots, L) \tag{36}$$

### 2.7 Weighting techniques

To obtain a global controller, the membership functions were developed from the map of a steady-state system (Figure 4). The weighting condition was derived from the membership functions. The values of weights in each region and intersection were calculated based on the average temperature of the multi-zone thermal plate system. The values of weights in each region and intersection are presented in Table 2.

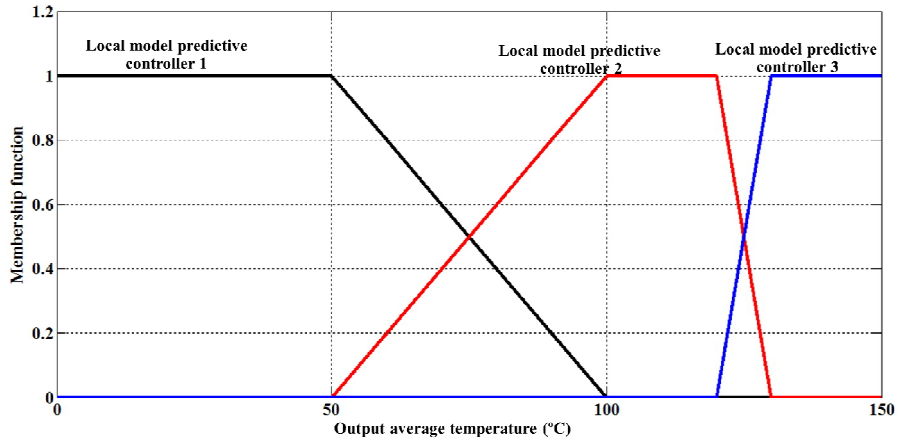


Figure 4. Membership function of a multi-zone thermal plate system.

Table 2. Values of weights in each region and intersection.

Average temperature ( $T_{ave}$ )	Weight condition		
	$W_1$	$W_2$	$W_3$
$T_{ave} < 50^\circ\text{C}$	1	0	0
$50^\circ\text{C} \leq T_{ave} < 100^\circ\text{C}$	$\frac{T_{ave}-50}{50-100}$	$1 - W_1$	0
$100^\circ\text{C} \leq T_{ave} < 120^\circ\text{C}$	0	1	0
$120^\circ\text{C} \leq T_{ave} < 130^\circ\text{C}$	0	$\frac{T_{ave}-120}{120-130}$	$1 - W_2$
$T_{ave} > 130^\circ\text{C}$	0	0	1

We checked the robust stability of the closed-loop multi-model system using the procedure of Gahinet *et al.* (1995) to find a common P from the LMI toolbox. The parameters  $N_p$  and  $N_c$  for the closed-loop matrix  $\tilde{Q}_{Ci}$ ,  $i \in (1, 2, 3)$  in the conventional case were selected to 10 steps and 5 steps and used the subscript C to represent the conventional case. The closed-loop matrices are presented as equation (37):

$$\begin{aligned}
 \tilde{Q}_{C1} &= \begin{bmatrix} 0.92 & 0.07 & -0.09 & 0.08 \\ 0.30 & 0.62 & -0.04 & 0.15 \\ 0.14 & 0.05 & 0.52 & 0.28 \\ 0.10 & 0.03 & 0.09 & 0.79 \end{bmatrix}, \tilde{Q}_{C2} = \begin{bmatrix} 0.90 & 0.01 & -0.01 & 0.10 \\ 0.15 & 0.65 & 0.01 & 0.17 \\ 0.07 & -0.04 & 0.73 & 0.15 \\ 0.10 & 0.10 & 0.06 & 0.77 \end{bmatrix} \\
 \tilde{Q}_{C3} &= \begin{bmatrix} 0.89 & -0.07 & -0.03 & 0.17 \\ 0.11 & 0.65 & 0.07 & 0.21 \\ 0.09 & 0.03 & 0.69 & 0.16 \\ 0.14 & 0.15 & 0.01 & 0.72 \end{bmatrix}
 \end{aligned} \tag{37}$$

From theorem 2, the common positive definite matrix  $p_c$  was found as:

$$P_c = \begin{bmatrix} 25.94 & -0.04 & -6.47 & 4.12 \\ -0.04 & 8.20 & -2.53 & -1.40 \\ -6.47 & -2.53 & 10.20 & -2.93 \\ 4.123 & -1.40 & -2.93 & 11.62 \end{bmatrix} \tag{38}$$

In the case of the robust model predictive controller, the vectors for the three operating temperature conditions of 60 °C, 65 °C and 75 °C were substituted into the linear matrix inequality to determine their robust controller. The closed-loop matrix  $\tilde{Q}_{Ri}$ ,  $i \in (1, 2, 3)$  in this case was drawn from equation (39). The subscript R represents a robust case.

$$\begin{aligned} \tilde{Q}_{R1} &= \begin{bmatrix} 0.90 & 0.06 & -0.09 & 0.08 \\ 0.25 & 0.58 & -0.04 & 0.15 \\ 0.10 & 0.04 & 0.51 & 0.28 \\ 0.07 & 0.03 & 0.09 & 0.79 \end{bmatrix}, \tilde{Q}_{R2} = \begin{bmatrix} 0.86 & 0.07 & -0.02 & 0.12 \\ 0.15 & 0.64 & 0.01 & 0.17 \\ 0.06 & -0.05 & 0.73 & 0.15 \\ 0.08 & 0.10 & 0.06 & 0.79 \end{bmatrix} \\ \tilde{Q}_{R3} &= \begin{bmatrix} 0.87 & -0.07 & -0.01 & 0.16 \\ 0.10 & 0.64 & 0.004 & 0.20 \\ 0.09 & 0.03 & 0.69 & 0.17 \\ 0.14 & 0.15 & 0.01 & 0.72 \end{bmatrix} \end{aligned} \tag{39}$$

From theorem 2, we found the common positive definite matrix  $P_R$  as:

$$P_R = \begin{bmatrix} 2.00 & -0.22 & -0.38 & 0.09 \\ -0.22 & 1.169 & -0.29 & -0.12 \\ -0.39 & -0.29 & 1.26 & -0.16 \\ 0.089 & -0.12 & -0.15 & 1.57 \end{bmatrix} \tag{40}$$

Then if the condition  $\tilde{Q}_i^T P \tilde{Q}_i - P < 0$  is satisfied for  $i \in (1,2,3)$  in the case of the conventional controller and the robust controller, the multi-model with uncertainties system is globally asymptotically stable.

### 2.8 Experimental set-up

Four thermocouples measured the temperature from each thermal zone. An IC AD595 was used to amplify weak temperature signals and a low-pass filter circuit was used to reduce the amplitude of the noise effect. An amplified temperature signal was used as feedback data to calculate error signals at the controller section. Two power devices were used to distribute 12 volt DC from the power supply to the thermoelectric plate in each zone when a control signal from the data acquisition card (Arduino MEGA 2560) was applied to the power device for a finite time. The computer and data acquisition card were connected via a USB cable. Then, a real-time hardware-in-the-loop experiment was performed using the MATLAB and Simulink programs. Experimentally, the conventional and the robust state feedback gain in the framework of the multi-model predictive control were compared. The average zone temperature in the multi-zone thermal plate system was used as the value for selecting the suitable controller gain based on the weighting condition to control a multi-zone thermal plate system intended for use over a wide range of operating conditions.

### 3. Results

#### 3.1 Simulation of a multi-zone thermal plate system

Simulation of the tracking performance of the multi-zone thermal plate system under multi-model predictive control (MMPC) and robust multi-model predictive control (RMMPC) is presented in Figure 5. A three-step change was used as the temperature reference signal for thermal zones 1 and 4, while two-level temperature reference signals were used for thermal zones 2 and 3. The results showed that using an RMMPC controller produced a better rise time in transient response of temperature in all thermal zones than MMPC. However, no difference in the closed-loop responses under a steady-state condition was found between the two controllers. During the first 50-second period, it was noted that average temperature changes in the case of RMMPC were smoother than for the MMPC (Figure 6A). The weight value of the first region local controller decreased, while that of the second region, based on the weight condition, increased as the average temperature exceeded 50 °C. Figure 6B shows fluctuations in the weight values in the MMPC during the first 50 seconds of the simulation. The values of weights 1 and 2 under the RMMPC case are shared as a smoother signal.

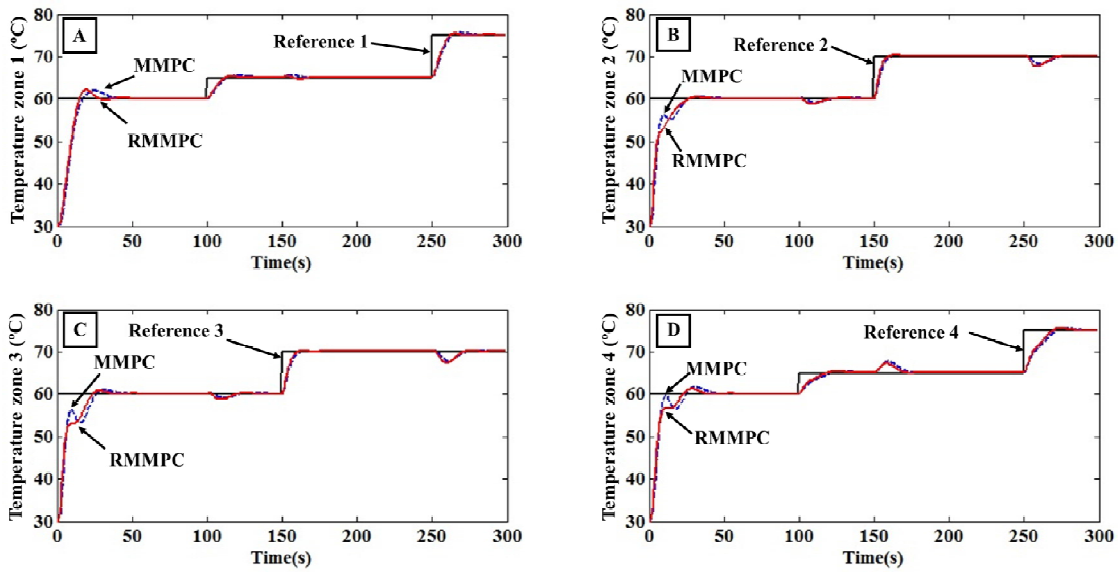


Figure 5. Tracking performance comparison between a multi-model predictive control (MMPC) and a robust multi-model predictive control (RMMPC) in a multi-zone thermal plates system: (A) Thermal zone 1; (B) Thermal zone 2; (C) Thermal zone 3, and (D) Thermal zone 4.

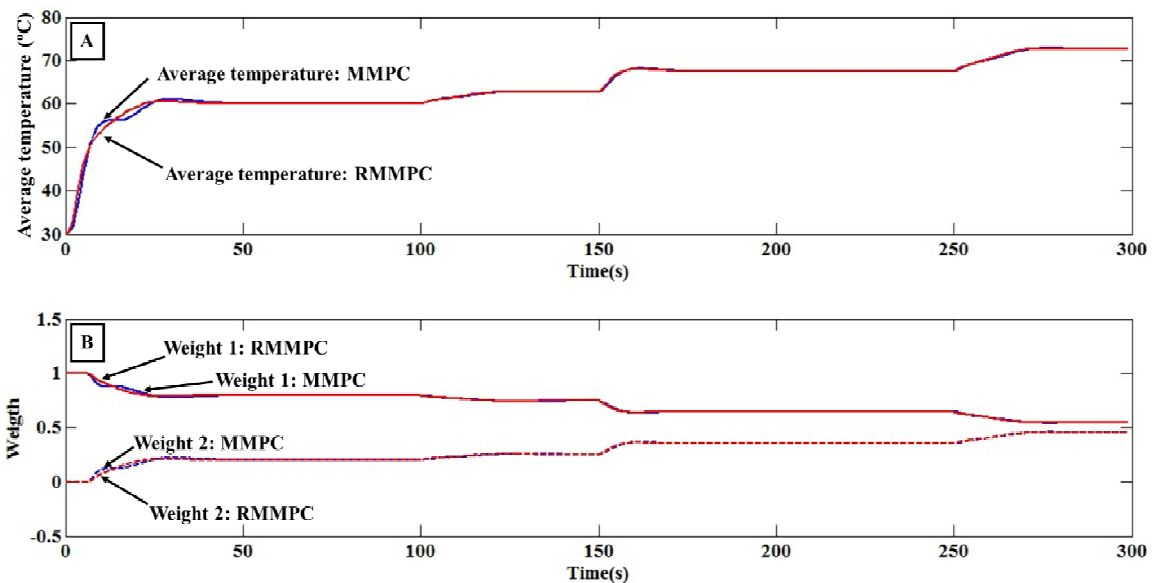


Figure 6. Simulation results: (A) Average temperature responses and (B) weight values.

### 3.2 Experimental results

Experimental tracking performance of the controllers in a multi-zone thermal plate system is presented in Figure 7. Solid and dashed lines represent the tracking performance of the RMMPC and MMPC, respectively. The transient responses of all temperature zones are better when using the RMMPC than the MMPC. When the system is working under steady-state conditions, the performance of both controllers is the same in thermal zones 1, 2, and 3. The temperature responses in thermal zone 4 could not track the

set-point during the last 50 seconds using the MMPC as a controller. The average temperature in the case of the MMPC was greater than in the RMMPC case during the first 50 seconds of the experiment (Figure 8A). Therefore, the weights 1 and 2 values decreased and increased faster than the weight values in the RMMPC case (Figure 8B).

After 50 seconds of the first period, the values of weights 1 and 2 were similar in the cases of both the MMPC and the RMMPC. In the last 50 seconds, weights 1 and 2 settled to 0.54 and 0.46, respectively.

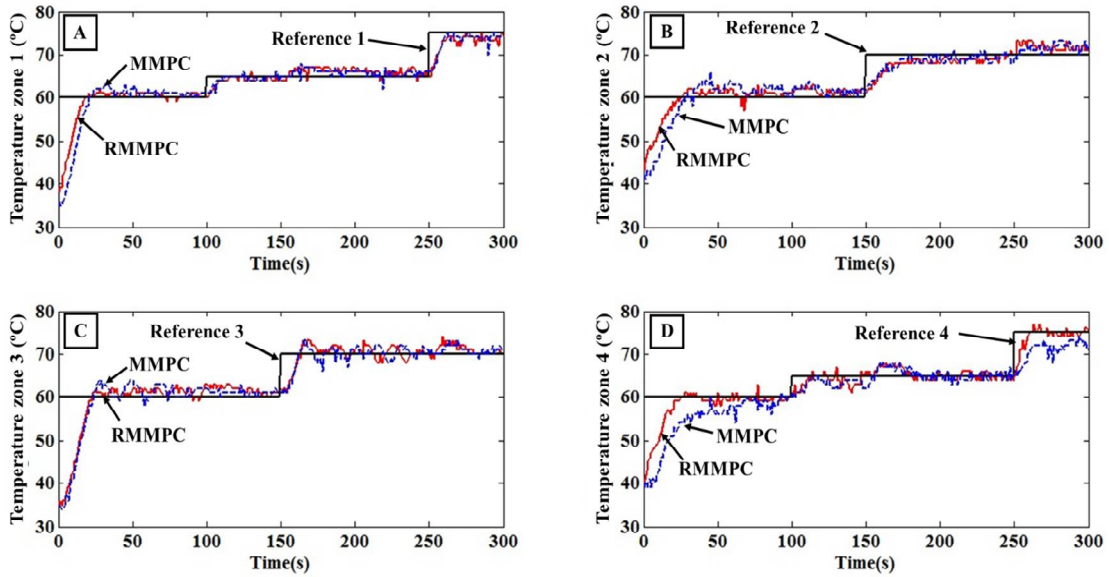


Figure 7. Experimental results of tracking the performance between multi-model predictive control (MMPC) and robust multi-model predictive control (RMMP) in a multi-zone thermal plate system: (A) Thermal zone 1; (B) Thermal zone 2; (C) Thermal zone 3, and (D) Thermal zone 4.

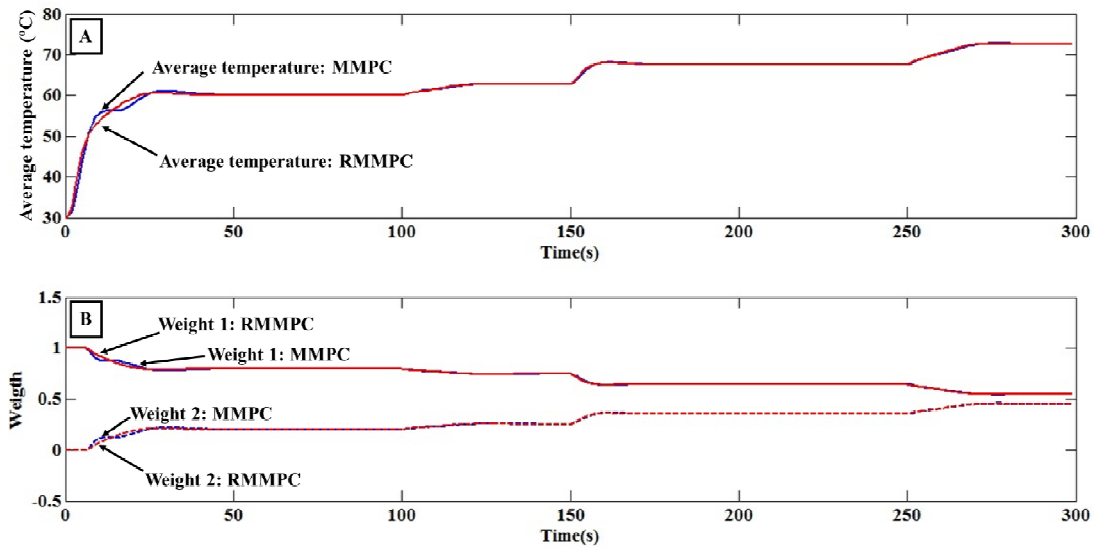


Figure 8. Experiment results: (A) Average temperature responses, and (B) weight values.

#### 4. Discussion

The robust model predictive controller in each of the operating conditions provided a better rise time in transient response than the conventional method in both the simulation and the experimental results. The weighting method of both cases made a smooth output signal for sharing the effects in each local controller.

The proposed controller is suitable for dealing with a wide range of operating conditions and system uncertainties. Therefore, a wide range of operating condition systems or variable load systems such as a refrigeration system, motor drive system, distillation column system, vehicle dynamic system, water tank system, and external forces system may use this proposed controller in cases of both single-input single-output and multi-input multi-output problems.

## 5. Conclusions

This paper has combined all local MPC and RMPC into a global controller using a weighting method. The design of the RMPC was based on parameter uncertainty in a multi-zone thermal plate system and the case of MPC was based on the conventional method. The design of the weighting method was based on the steady-state map of a multi-zone thermal plate system. The weight condition was suitable for sharing the effects of each local controller according to the average temperature value. We derived stability in both cases of MPC and RMPC to ensure the stability property.

As a comparison study, the proposed controller and conventional method were substantiated by simulation and experiment on a multi-zone thermal plate system. Simulation and experimental results showed that the proposed controller demonstrated improvement on the transient performance of the closed-loop system. Future work will focus on constrained problems in this control system.

## References

- Chen, Q., Gao, L., Dougal, R. A., & Quan, S. (2009). Multiple model predictive control for a hybrid proton exchange membrane fuel cell system. *Journal of Power Sources*, 191(2), 473–482.
- Dougherty, D., & Cooper, D. (2003). A practical multiple model adaptive strategy for multivariable model predictive control. *Control Engineering Practice*, 11(6), 649–664.
- Gahinet, P., Nemirovski, A., Laub, A. J., & Chilali, M. (1995). *LMI toolbox for use with MATLAB*. Natick, MA: The Mathwork.
- Gan, L., & Wang, L. (2011). A multi-model approach to predictive control of induction motor. *IECON 2011 – 37<sup>th</sup> Annual Conference on IEEE industrial Electronics Society* 37, 1704–1709.
- Hamane, H., Matuki, K., Hiroki, F., & Miyazaki, K. (2010). Thermal MIMO controller for set point regulation and load disturbance rejection. *Control Engineering Practice*, 18(2), 198–208.
- Ho, W. K., Tay, A., Cheng, M., & Kiew, C. M. (2007). Optimal feed-forward control for multi-zone baking in microlithography. *Industrial and Engineering Chemistry Research*, 46(11), 3623–3628.
- Kothare, M. V., Balakrishnan, V., & Morari, M. (1996). Robust constrained model predictive control using linear matrix inequalities. *Automatica*, 32(10), 1361–1379.
- Ling, K. V., Ho, W. K., Wu, B. F., Andreas, L. O., & Yan, H. (2009). Multiplexed MPC for multi-zone thermal processing in semiconductor manufacturing. *IEEE Transaction on Control System Technology*, 18(6), 1371–1380.
- Maciejowski, J. M. (2002). *Predictive Control with Constraints*. Upper Saddle River, NJ: Prentice-Hall Publishing.
- Tanaka, K., & Sugeno, M. (1992). Stability analysis and design of fuzzy control systems. *Fuzzy Sets and Systems*, 45, 135–156.
- Tan, W., Horacio, H., Marquez, J., & Chen, T. (2004). Operating point selection in multi-model controller design. *American Control Conference 2004*, 3652–3657.
- Tay, A., Ho, W. K., Schaper, C. D., & Lee, L. L. (2004). Constraint feedforward control for thermal processing of quartz photomasks in microelectronics manufacturing. *Journal of Process Control*, 14, 31–39.
- Tay, A., Chua, H. T., Yuheng, W., Geng, Y., & Ho, W. K. (2013). Modeling and real-time control of multizone thermal processing system for photoresist processing. *Industrial and Engineering Chemistry Research*, 52(13), 4805–4814.
- Wang, L. (2009). *Model Predictive Control System Design and Implementation Using MATLAB*. London, England: Springer-Verlag.